Adsorption (2012) 18:493–501
DOI 10.1007/s10450-012-9439-6

Adsorption, diffusion and catalysis of mesostructured zeolite HZSM-5

Zhiping Liu · Weiming Fan · Jinghong Ma · Ruifeng Li

Received: 22 May 2012 / Accepted: 4 October 2012 / Published online: 24 October 2012

Abstract Adsorption and diffusion properties of *n*-octane in meso-structured HZSM-5 zeolites were studied by high precision intelligent gravimetric analysis (IGA) and ZLC technology between 293 K and 393 K. As expected, great increase in adsorption capacity and diffusion efficient of *n*-octane in the mesostructured HZSM-5 zeolites was observed compared with conventional HZSM-5. At the same time, the adsorption activation energy of *n*-octane in the mesostructured HZSM-5 zeolites was significantly decreased. The adsorption heats with low *n*-octane loading showed a clear decline with increase of mesoporosity in the zeolite samples. These results clearly indicate that introduction of mesopores into the zeolites offered a short diffusion path and high diffusion rate for reactants and products, which resulted in a high yield of fuel oil and an enhanced resistance against the catalyst deactivation in the reaction of methanol to gasoline.

Keywords Mesostructured zeolite HZSM-5 · Adsorption isotherm · Diffusion kinetics · Activation energy

1 Introduction

Methanol-to-gasoline (MTG) reaction based on HZSM-5 zeolite catalysts offers a new and practical route for producing high quality gasoline. However, one of the major issues for commercial application of the MTG process is relatively fast deactivation of the catalyst because of the formation of carbonaceous species. It seems to be a consensus that slow adsorption/desorption and pore-diffusion of the reactants and products are the causative factors for catalyst deactivation. The small microporous channels in zeolite heavily hinder the mass transfer by limiting diffusion rate, especially when the reaction is significantly faster than diffusion in the micropores (Corma 1997; van Donk et al. 2003; Egeblad et al. 2008; Groen et al. 2004a, 2004b; Gong et al. 2009; Karger and Ruthven 1992). As a result, it is highly needed to develop a new material with hierarchically porous architecture (Choi et al. 2006; Corma 1997; Soler-Illia et al. 2002; Tao et al. 2006; Xiao et al. 2006). The larger pores facilitate transportation of reaction molecules, whereas each micropore acts as a nanoreactor providing active sites and shape selectivity (Groen et al. 2007; Holmberg et al. 2003; Su et al. 2003).

For a given zeolite framework , the basic strategy to change the diffusion path length is to alter crystal size and morphology using particularly crystallization conditions (Groen et al. 2007; Jacobsen et al. 2000; Perez-Ramirez et al. 2008; Serrano et al. 2009). Another approach is to insert larger pores into the zeolite particles, since the diffusion in mesopores is several orders of magnitude faster than in micropores. Among these, an innovative post-treatment method, desilication or base leaching, has attracted extensive attention owing to the creation of a network of micropores and mesopores.

The diffusion capability of large molecules in zeolite channels can be improved by introduction of mesoporous structures, thus the zeolite catalyst has excellent catalytic property. Catalysis of polyethylene showed hierarchical HZSM-5 exhibited three times higher activity than conventional HZSM-5 (Aguado et al. 2008; Serrano et al. 2008,

Z. Liu · R. Li (✉)
College of Chemistry and Chemical Engineering, Taiyuan University of Technology, Taiyuan, 030024, China
e-mail: ruifeng_li@hotmail.com

W. Fan · J. Ma (✉) · R. Li
Key Laboratory of Coal Science and Technology MOE, Institute of Special Chemicals, Taiyuan, 030024, China
e-mail: majinghong@hotmail.com

2009). Groen et al. (2007) reported a pioneering work in which they provided directly experimental evidence to mesoporous ZSM-5 zeolite. The characteristic diffusion path length in the mesoporous crystals was dramatically shortened, resulting in an approximately two orders of magnitude faster diffusion of neopentane in the majority of micropores. The diffusion coefficient of cumene increased by 2–3 orders of magnitude and the diffusion-adsorption activation energy increased by a factor of 4.6 with the introduction of mesoporous structure to ZSM-5.

Despite many efforts in synthesis, characterization, and catalytic evaluation of the mesostructured HZSM-5 materials, the logical relationship between diffusion rate of such molecules and catalytic reaction has still been highly debatable (Zhao et al. 2008). The corresponding reports investigating the adsorption and diffusion characteristics of reactants and products in the micro-mesoporous zeolite crystals are few.

In order to better understand the relation among adsorption, diffusion and catalytic behavior and obtain thermodynamic and dynamic parameters correlating adsorption, diffusion and catalysis, here, mesostructured HZSM-5 zeolites were prepared by base leaching method. The experimental adsorption isotherms and diffusion kinetic curves presented to investigate the structure and related diffusion properties of the zeolits with different mesoporosity at different temperatures. Simultaneity, diffusion efficient in the zeolites was determined for directly evidence of the catalytic conversion of methanol-to-gasoline (MTG) on the zeolite catalysts.

The adsorption isotherms are measured by a high precision intelligent gravimetric analyzer (IGA), while the diffusion dynamics are investigated using the zero length column (ZLC) technique. *n*-Octane is selected as a probe molecule because it is one component of gasoline, the kinetics diameter is similar to the channel openings of HZSM-5, allowing accurate assessment of diffusion rates. The physical-chemical characterizations associated with the adsorption and diffusion property evaluations provide necessary information for a better understanding of the potential for gas separation, adsorption and catalytic process using zeolite/mesostructured materials (Bárcia et al. 2005; Da Silva and Rodrigues 1999; Vinh-Thang et al. 2006), in particular, mesostructured HZSM-5 materials.

2 Experimental section

2.1 Preparation of samples

A commercially available ZSM-5 zeolite provided by Fushun Research Institute of Petroleum and Petrochemicals of China was used as standard material (designated as ZSM-5(0)). ZSM-5(0) zeolite sample was alkali treated separately in 0.5, 0.7 and 0.9 M NaOH solution and stirred at 333 K for 360 min. The resulted samples were filtered and washed with distilled water until a neutral pH, and then dried at 373 K overnight. Then the alkali-treated samples were ion exchanged with 0.5 M NH_4NO_3 aqueous solution and stirred at 303 K for 180 min, followed by filtering and rinsing with distilled water to remove sodium ions. This procedure was repeated three times to obtain NH_4-ZSM-5. The samples were then calcined in air at 773 K to obtained HZSM-5 (denoted as HZSM-5(x) ($x = 1, 2, 3$), where x is corresponding to the alkali concentration).

2.2 Characterization

The XRD patterns were recorded using a SHIMADZU XRD-6000 X-ray diffractometer operated at 40 kV and 30 mA, which employed Ni-filtered and Cu Kα radiation. Crystal size, morphology and mesoporous structure of the samples were investigated using SEM on a JEOL/JSM-6700F scanning electron microscope.

N_2 adsorption at 77 K was performed in a NOVA 1200e gas sorption analyzer to study the micro- and mesoporosity in the zeolite crystals. The mesopore size distribution was calculated using the Barret–Joyner–Halenda (BJH) pore size model based on the adsorption branch of the isotherm. The microporous structure was obtained from the t-plot analysis of the adsorption branch of the isotherm.

The variation of acidity of the HZSM-5 zeolites by the alkali treatment was investigated by using Temperature-programmed desorption of ammonia (NH_3-TPD). About 70 mg of catalyst was loaded in a quartz U-tube and supported by quartz wool. Then, it was treated at 823 K for 3 h in a highly purified He (99.999 %) flow. After cooled down to 393 K, the sample was saturated with a NH_3 (10 %)/He gas mixture, followed by purging with the highly purified He for an hour at 393 K. Then, the temperature was increased at a rate of 10 K/min in a highly purified He flow (80 ml/min). The desorption of NH_3 was monitored by using a thermal conductivity detector.

2.3 Adsorption isotherm measurements

Adsorption isotherms of *n*-octane over the mesostructured HZSM-5 samples were measured by using a high precision intelligent gravimetric analyzer (IGA). A sensitive microbalance (resolution of 0.1 μg) was mounted in a thermostat which was used as an enclosure to remove thermal coefficients of the weighing system and thus give a higher stability and accuracy. A small amount of the sample (40–60 mg) was loaded in the microbalance basket submitted to a controlled temperature ramp of 0.1 K/min in vacuum conditions (total pressure of less than 10^{-6} mbar) until reaching 693 K. The sample was kept at 693 K and 10^{-6} mbar for 8–10 h prior to the adsorption measurement. The sample temperature was regulated within 0.1 K by either a water bath or

a furnace. For each step, the amount of sorbate introduced into the system was kept small enough to keep the adsorption process isothermal (Zhao et al. 2008). The increase of weight was continuously recorded. The pressure was determined by two high accuracy Baratron pressure transducers. The dosing continued until the entire equilibrium adsorption isotherm was obtained.

2.4 Diffusion measurement

The n-octane diffusion in the mesostructured HZSM-5 samples was investigated by a ZLC method (Eic and Ruthven 1988). The ZLC was prepared by sandwiching a small quantity of adsorbent (1–2 mg) between two porous sinter discs held within a Swagelok 1/8 in. fitting. The ZLC column and switching valve were placed in a gas chromatograph oven (Agilent 1790). The flow rates were controlled by mass flow controllers. A small amount of sample powder was loaded into the ZLC column and activated at 300 °C overnight in pure helium (99.99 %) to eliminate impurities and moisture in particular. After the sample was cooled and reached the measurement temperature, and corresponded to the linear region of the adsorption isotherm (Henry's Law region), the carrier gas (helium or argon) containing a very low concentration of n-octane (99 % grade, Aldrich, partial pressure 0.04 mbar) was passed through the sample column at a high flow rate until it was saturated as confirmed by monitoring the effluent stream by FID. Then a four-way valve was switched (at time zero), a pure carrier gas at the same rate was fed to the ZLC, the adsorbent was purged. The time-dependent effluent concentration of n-octane was measured by FID and recorded automatically by the GC, and was used to evaluate the effective diffusivity (Gobin et al. 2007; Gunadi and Brandani 2006; Vinh-Thang et al. 2006).

For each experimental condition, 2–3 different flow rates were adopted in the range of 50–100 cm^3/min to confirm the kinetically controlled process. A purge flow rate of 85 cm^3/min helium was then chosen as a standard flow rate for all experiments in this study.

In the case of uniform spherical particles being in linear adsorption equilibrium at very low sorbate partial pressures, neglecting the hold up in the ZLC bed and assuming perfect mixing throughout the ZLC cell, the normalized effluent sorbate concentration c/c_0 is described by the following set of equations (Bárcia et al. 2005; Gobin et al. 2007).

$$\frac{c}{c_0} = 2L \sum_{n=1}^{\infty} \frac{\exp(-\beta_n^2 D_{\text{eff}} t/R^2)}{\beta_n^2[\beta_n^2 + L(L-1)]} \tag{1}$$

$$L = \frac{1}{3}\frac{F}{KV_s}\frac{R^2}{D_{\text{eff}}} \tag{2}$$

$$\beta_n \cot \beta_n + L - 1 = 0 \tag{3}$$

Where β_n is given by the roots of Eq. (3), K is the dimensionless Henry law constant and D_{eff}/R^2 is effective diffusion time constant.

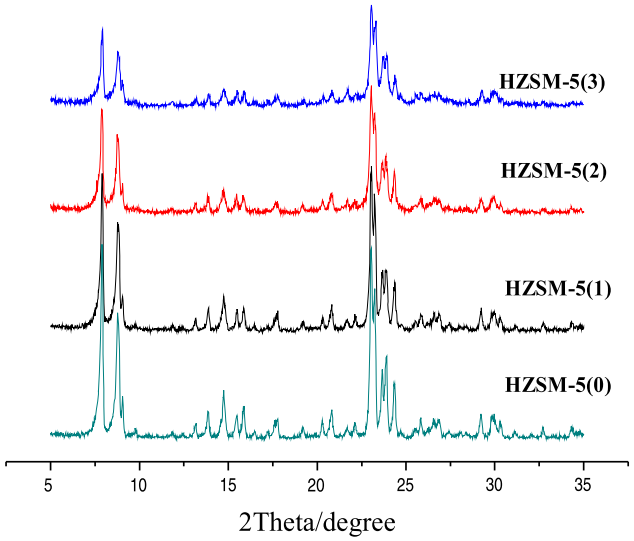

Fig. 1 XRD patterns of different samples. (**a**) HZSM-5(0); (**b**) HZSM-5(1); (**c**) HZSM-5(2); (**d**) HZSM-5(3) zeolites

2.5 Catalytic testing

All catalytic experiments were conducted at atmospheric pressure in a fixed-bed micro-reactor (Newford) with a stainless tube (i.d. 12 mm). Prior to each experiment, the H-zeolite sample was pressed into a cylinder and then broken into 20–40 mesh particles and activated under the flowing N_2 (50 ml/min) at 823 K for 2 h and then kept at desired reaction temperature. Methanol to gasoline reaction was carried out at 643 K with a WHSV of 4–8 g^{-1} h^{-1}. Gas products were analyzed by an online gas chromatograph with an FID detector and a GDX-101 column, while liquid products were analyzed by a gas chromatograph with an FID detector and a capillary column Rtx-1 (30 m × 0.25 mm × 0.25 μm).

3 Results and discussion

3.1 Preparation and characterization

Figure 1 is XRD patterns of HZSM-5(0) and HZSM-5(x) ($x = 1, 2, 3$). It can be observed that the topological structure of ZSM-5 zeolite is still retained in the samples after alkali-treatment and ion-exchange. The position of characteristic diffraction peaks of zeolite do not change, but the intensity of most peaks decrease with the increase of alkali concentration because of the removal of silicon species or/and silicon-aluminum species from the framework of ZSM-5 zeolites, without complete destruction of the crystal lattices.

Scanning electron microscope (SEM) images confirm the generation of intracrystalline mesoporosity in the alkali-treatment samples. As shown in Fig. 2, the morphology of HZSM-5(x) is very different from that of HZSM-5(0),

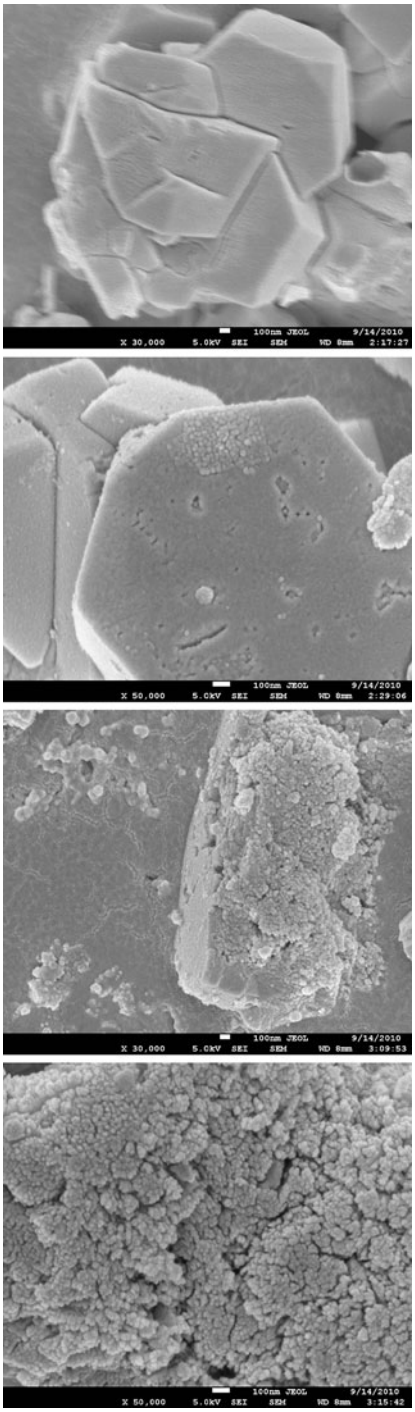

Fig. 2 High resolution TEM images of the samples. (**a**) HZSM-5(0); (**b**) HZSM-5(1); (**c**) HZSM-5(2); (**d**) HZSM-5(3) zeolites

which possesses classical coffin-like morphology of MFI zeolite. After alkali-treatment, the zeolites are perforated by pronounced dissolution, resulting in the formation of about 2–50 nm mesopores and wide entrances to the center of the crystals. However, the profiles of zeolite particles are the characteristic shape of the MFI zeolite.

N_2 adsorption isotherms on the HZSM-5(0) and HZSM-5(x) ($x = 1, 2, 3$) zeolite samples reveal that various hierarchical pores are formed upon alkali-treatment. As shown in Fig. 3, the untreated sample (HZSM-5(0)) shows type I isotherm which is typical of microporous materials, while HZSM-5(x) zeolite exhibits significantly higher N_2 adsorption amount at both intermediate and high relative pressures than HZSM-5(0) zeolite, indicating that HZSM-5(x) samples possess much higher porosities and special surface areas. According to the results of porous properties of the zeolites summarized in Table 1, S_{BET}, S_{EX} and mesoporous volume (V_{meso}) increase after alkali treatment, indicating that alkali-treatment technique yielded a zeolite with mesoporous structure (Zhao et al. 2008).

The removal of silicon atoms from skeletal during the alkali treatment increases the number of acid sites. The destruction of zeolite structure causes the loss of strong acid sites (Jung et al. 2005). Figure 4 shows TPD profiles of ammonia on the alkali-treated HZSM-5 zeolites, indicating the number of strong acid sites on the HZSM-5(3) zeolite decreases clearly.

3.2 Adsorption isotherms

The adsorption isotherms of n-octane on four HZSM-5 zeolites with different mesoporosity were obtained at 20, 35 and 45 °C , respectively. As shown in Fig. 5, the isotherms of HZSM-5(0) at different temperatures show a typical Langmuir Type-I adsorption, which reaches saturation at a low pressure and then increases slightly with the increase of pressure. However, the isotherms for mesostructured HZSM-5(x) show a completely different trend from these of HZSM-5(0). The characteristics of type-I and type-IV at the same time suggest the formation of some mesoporous structures. The adsorption capacities of HZSM-5(x) zeolites are always higher than HZSM-5(0) over the range of pressure. The adsorption amount of n-octane on HZSM-5(x) continuously increases along with pressure. The saturation adsorption capacities of n-octane in HZSM-5(x) are higher than that in HZSM-5(0) zeolite, agreeing well with BET characterization results, i.e. after the introduction of mesoporous, the total surface area of mesostructured HZSM-5 zeolites is approximately 14 % higher than that of HZSM-5(0) zeolite.

The adsorption heat is a measure of interaction between zeolite surface and adsorbate molecules. The amount of the adsorption heat is evaluated from the temperature dependence of adsorption data, using the Clausius-Clapeyron equation. At low n-octane loading, the dependence of adsorption heats of n-octane on the samples relates to the mesoporosity. At the limited zero-loading, the adsorption heat of n-octane on the HZSM-5(0) zeolite is about 65 kJ/mol, while in the same condition the adsorption heat

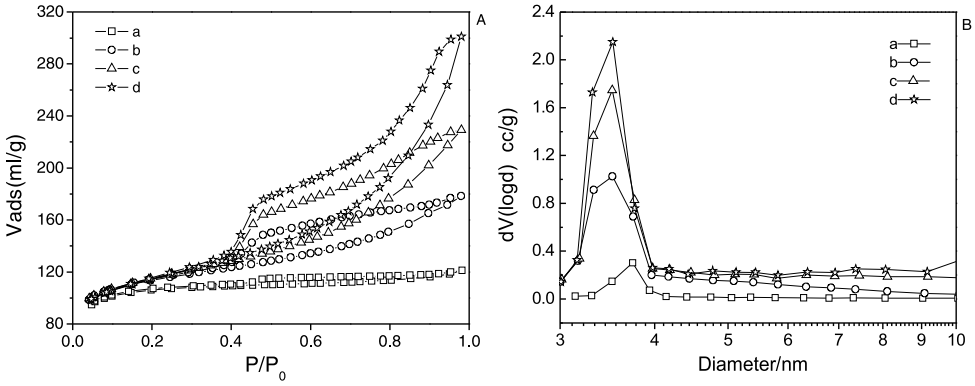

Fig. 3 Nitrogen adsorption isotherms at 77 K. (*a*) HZSM-5(0); (*b*) HZSM-5(1); (*c*) HZSM-5(2); (*d*) HZSM-5(3) zeolites

Table 1 The porous properties of the HZSM-5 and Meso-structured HZSM-5 zeolites

Catalyst	Si/Al (bulk)	S_{BET} (m^2/g)[a]	S_{EX} (m^2/g)[b]	V_{micro} (cm^3g^{-1})[b]	V_{meso} (cm^3g^{-1})[c]
HZSM-5(0)	36	326	57	0.14	0.03
HZSM-5(1)	31	362	130	0.12	0.15
HZSM-5(2)	28	371	163	0.11	0.25
HZSM-5(3)	23	373	192	0.09	0.39

[a]BET surface area obtained from N_2 adsorption isotherm in the relative pressure range of 0.05–0.30

[b]Micoropore volume was calculated from the *t*-plot method

[c]Mesopore volume was calculated from the BJH method

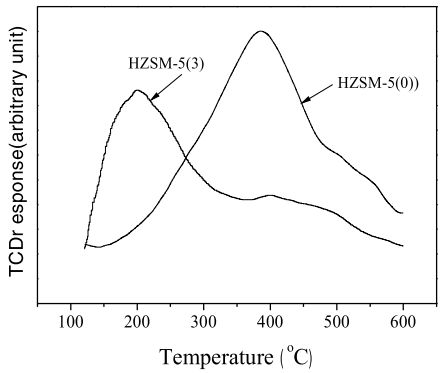

Fig. 4 TPD profiles of ammonia from alkali-treated HZSM-5 zeolites

on the HZSM-5(3) is 30 kJ/mol. The adsorption heat decreased with increasing *n*-octane coverage on the two samples. This can be explained by the fact that the heat released from different adsorption sites varies, owing to the difference in the energy of the surface adsorption sites (Zhao et al. 2008). The strong adsorption sites result in high adsorption heat and *vice versa*. The conventional micropore HZSM-5(0) gave the highest adsorption heat of *n*-octane, because its stronger adsorption sites resulted in strong interaction between the sites and the adsorbent. *n*-Octane is adsorbed on relatively weak adsorption sites of the mesostructured zeolites, the adsorption heat is relatively low (Kang et al. 2011), which is related to acid sites of the surface on the zeolites (Fig. 4). However, the heat of adsorption at low loading showed a decrease trend with increase of mesoporosity in the mesostructured zeolites. Combined with the results obtained from NH_3-TPD, an explanation for such behavior is suggested, by which the strong acid sites of the sample decreased significantly after alkali treatment, while the amount of weak acid sites increased obviously. *n*-Octane was adsorbed mainly on the relatively weak sites of mesostructured HZSM-5 zeolite, resulting in decreased adsorption heat.

In order to investigate the effect of mesoporosity (see Table 1) on diffusivity and to verify the improved transport properties of mesostructured HZSM-5 zeolites, four HZSM-5 zeolites with different mesoporosity were investigated by using the ZLC method.

The experimental ZLC desorption curves of *n*-octane in different mesoporosity HZSM-5 zeolites at different temperatures are fitted by the ZLC model as shown in Fig. 6. Figure 5 displays the adsorption isotherms of *n*-octane on the samples at different temperatures, confirming that the ZLC experiments are conducted in the linear region of isotherms as required by the ZLC theory. The runs were performed at 85 and 70 ml/min, yielding *L* values far higher than 5 (*L* value generally greater than 5 is used as a criterion), which ensures that the system is kinetically controlled (Brandani et al. 2000; Jiang and Eić 2003). Good agreement between experimental data and the model fits

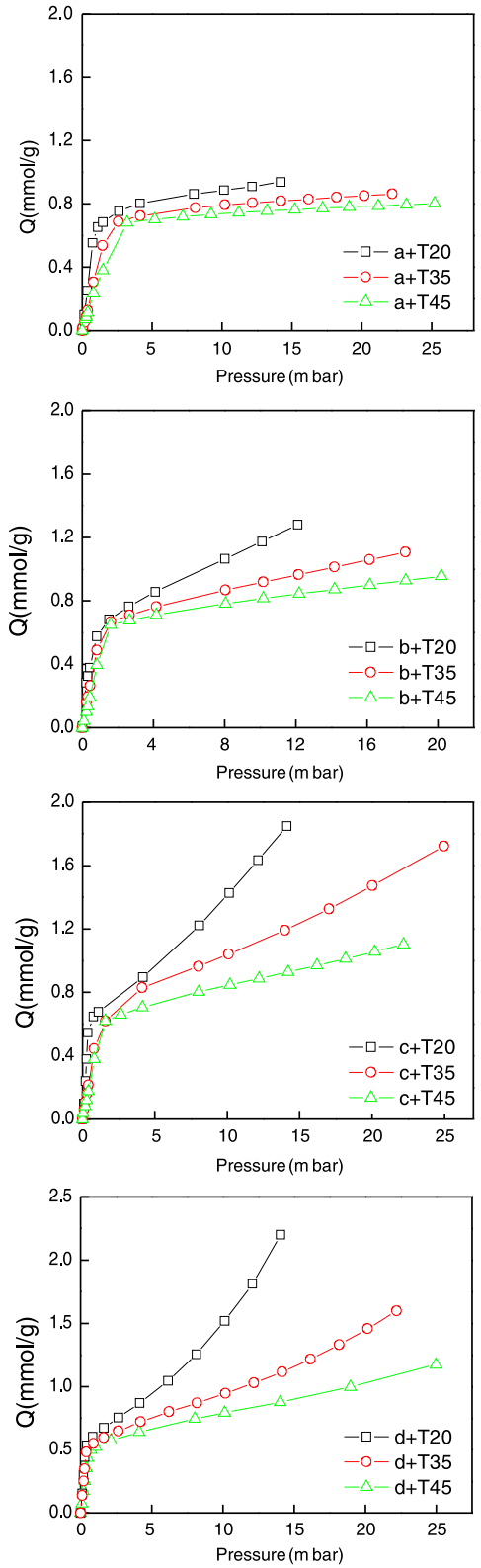

Fig. 5 Adsorption isotherms of *n*-octane on zeolites at various temperatures: (**a**) HZSM-5(0); (**b**) HZSM-5(1); (**c**) HZSM-5(2); (**d**) HZSM-5(3)

Table 2 Diffusivity Data of *n*-Octane for different samples

Sample	T (°C)	L	D_{eff}/R^2 (10-4)	Ea (kJ/mol)
HZSM-5(0)	60	29.5	1.10	25.6
	45	31.2	0.70	
	35	22.0	0.52	
HZSM-5(1)	60	23.7	1.11	21.0
	45	31.3	0.80	
	35	22.1	0.60	
HZSM-5(2)	60	26.8	1.30	15.7
	45	30.7	1.04	
	35	28.4	0.81	
HZSM-5(3)	60	29.7	1.42	15.1
	45	34.8	1.11	
	35	29.5	0.91	

can be clearly observed. The values of the effective diffusion time constant (D_{eff}/R^2) extracts from the model fitting of the experimental ZLC curves together with the corresponding L values are listed in Table 2. Effective diffusion time constant (D_{eff}/R^2) increases with the temperature and mesoporosity for all measured samples as expected. This indicates that the introduced mesoporosity in the zeolites significantly accelerates the diffusion rate. Effective activation energy decreased from 25.6 to 15.1 kJ/mol after mesopores were introduced into the HZSM-5 zeolites, in which the reduction of adsorption energy barrier was beneficial to the transportation (Vinh-Thang et al. 2006; Zhao et al. 2008). The transport of *n*-octane in meso-HZSM-5(x) samples occurs in micropores and in mesopores, but the diffusion processes only in micropores in the conventional HZSM-5(0). A new transport mechanism that combines mesopore diffusion (the classical Knudsen diffusion) among the microporous crystalline is proposed although the diffusion limitation is still in the micropores. Because of the contribution of mesopore diffusion to the over mass transfer, it is reasonable that the extracted activation energy in meso-HZSM-5(x) samples is less than that in the HZSM-5(0) (Vinh-Thang et al. 2006). As can be drawn from Fig. 5 and Table 2, the alkali treatment of zeolite has enhanced both the diffusion rate and the amount of o-octane uptake on the HZSM-5 zeolites by forming mesopores, while the zeolitic structure is maintained. At the same time, the decreased adsorption heat suggests the decreased interaction between the zeolite surface and adsorbate molecules because the strong sites of samples are significantly decreased, and consequently products are released more rapidly.

3.3 Methanol to gasoline reaction

HZSM-5 is an advantaged catalyst in the MTG (methanol-to-gasoline) reaction. However, this catalyst deactivates

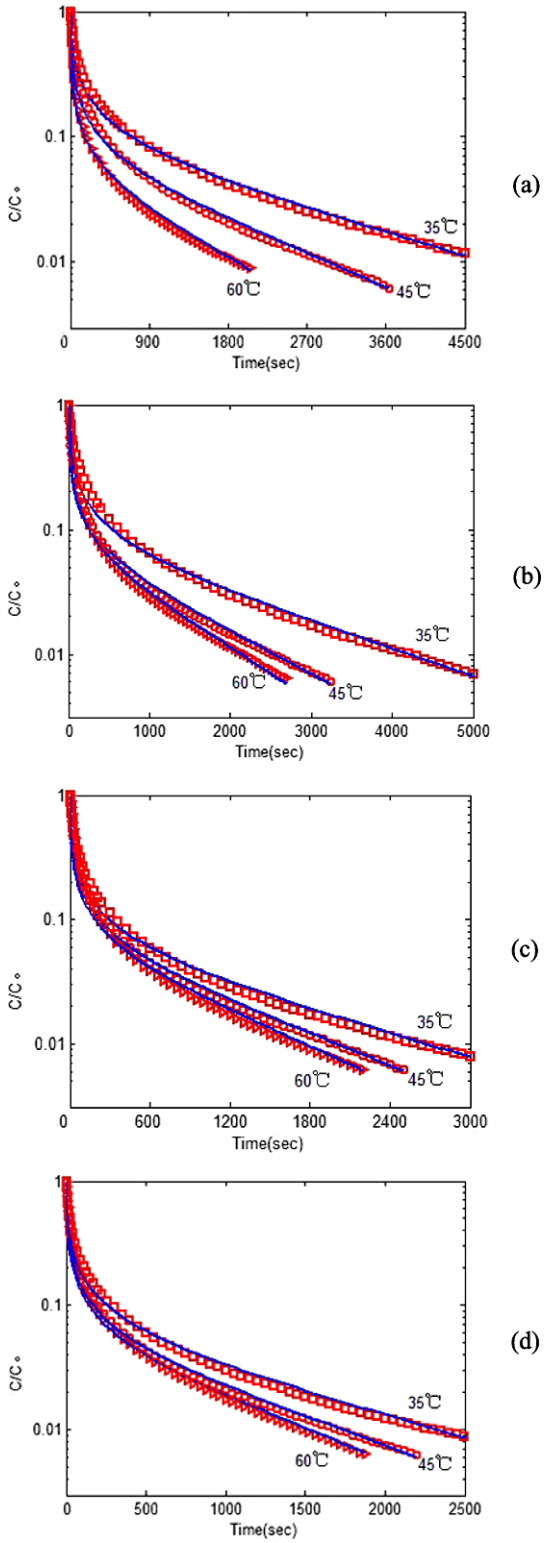

Fig. 6 Diffusivity data for *n*-octane in different samples: (**a**) HZSM-5(0); (**b**) HZSM-5(1); (**c**) HZSM-5(2); (**d**) HZSM-5(3) zeolites

rapidly because channel restriction results in slow pore diffusion of the products, which impacts on industry application. Here, the MTG reaction over HZSM-5(x) and HZSM-5(0) was performed at 643 K in a fixed bed reactor, and the results are displayed in Fig. 7. All samples indicate efficient catalytic performance in the methanol dehydration reaction and the meso-structured HZSM-5(x) zeolites exhibit a significantly higher conversion rate and selectivity toward the desired hydrocarbons than HZSM-5(0). Initial methanol conversion on HZSM-5(0) presents 89 %, however the conversions on the HZSM-5(x) are close to 99 %. Within 10 h, HZSM-5(0) deactivates rapidly and the methanol conversion reduces sharply to lower than 80 %. Whereas HZSM-5(3) keeps high methanol conversion for more than 20 h, and decreases to lower than 80 % after 45 h. With the increase of surface area of the samples by the introduction of mesopores into the microporous zeolite, more active sites are exposed to reactants and diffusion path length is decreased obviously, resulting in the higher conversion rate and longer catalyst life. Therefore, the introduction of mesopore would be among the most important factors to obtain an active and stable catalyst (Xue et al. 2012).

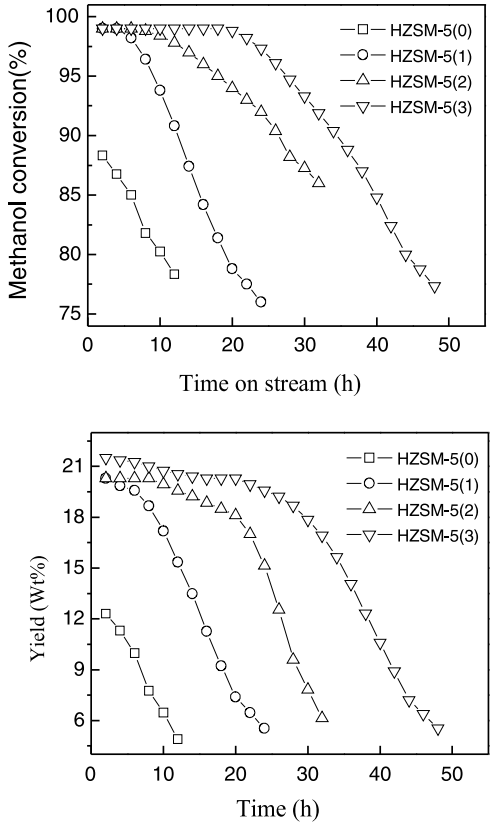

Fig. 7 **A**: The methanol conversion of HZSM-5(0) and HZSM-5(x) catalysts

In terms of yields, the fuel yields over HZSM-5(x) catalysts are significantly higher than that over HZSM-5(0). The yield of fuel oil on HZSM-5(3) is up to 22 % and keeps for 30 h. However, the yield of fuel oil on the HZSM-5(0) catalyst is only 12 % initially and then decreases to 5 % within 12 h. Owing to the existence of intracrystalline mesopores,

HZSM-5(3) offers a short diffusion path and a high diffusion rate. The facts are resulting in a high yield of fuel oil and lower cracking probability of long chain hydrocarbons to lighter paraffins, thus enhancing the resistance of the catalyst against deactivation.

4 Conclusions

In this study, HZSM-5(x) zeolites with different mesoporosity were prepared by alkaline treatment. From the diffusion data of n-octane, it showed that both the adsorption capacity and the effective diffusion time constant (D_{eff}/R^2) on mesopore structured HZSM-5 increased compared with conventional HZSM-5 zeolite, while activation energy decreased. The experimental results clearly indicated a facilitated process in HZSM-5(x) zeolites caused by the influence of mesopore as the main channel structure. The enhanced stability of the catalysts is resulted from the more facile desorption and faster diffusion of product molecules from the sites in micropores to the external surfaces of the mesopores owing to a large external surface area and short diffusion paths. The mesoporous structure in the zeolite samples decreased the probability of product cracking and coking, therefore, led a longer catalytic activity and higher yield of gasoline in the conversion of methanol to gasoline.

Acknowledgements This work was financially supported by "The National Nature Science Foundation of China" (Grant no. 50872087) and "Research Fund for the Doctoral Program of Higher Education of China" (No. 20111402110005).

References

Aguado, J., Serrano, D.P., Rodríguez, J.M.: Zeolite beta with hierarchical porosity prepared from organofunctionalized seeds. Microporous Mesoporous Mater. **115**, 504–513 (2008)

Bárcia, P.S., Silva, J.A.C., Rodrigues, A.E.: Adsorption equilibrium and kinetics of branched hexane isomers in pellets of BETA zeolite. Microporous Mesoporous Mater. **79**, 145–163 (2005)

Brandani, S., Jama, M.A., Ruthven, D.M.: ZLC measurements under non-linear conditions. Chem. Eng. Sci. **55**, 1205–1212 (2000)

Choi, M., Cho, H.S., Srivastava, R., Venkatesan, C., Choi, D.H., Ryoo, R.: Amphiphilic organosilane-directed synthesis of crystalline zeolite with tunable mesoporosity. Nat. Mater. **5**, 718–723 (2006)

Corma, A.: From microporous to mesoporous molecular sieve materials and their use in catalysis. Chem. Rev. **97**, 2373–2420 (1997)

Da Silva, F.A., Rodrigues, A.E.: Adsorption equilibria and kinetics for propylene and propane over 13X and 4A zeolite pellets. Ind. Eng. Chem. Res. **38**, 2051–2057 (1999)

Egeblad, K., Christensen, C.H., Kustova, M., Christensen, C.H.: Templating mesoporous zeolites. Chem. Mater. **20**, 946–960 (2008)

Eic, M., Ruthven, D.M.: A new experimental technique for measurement of intracrystalline diffusivity. Zeolites **8**, 40–45 (1988)

Gobin, O.C., Huang, Q.L., Thang, H.V., Kleitz, F., Eic, M., Kaliaguine, S.: Mesostructured silica SBA-16 with tailored intrawall porosity part 2: diffusion. J. Phys. Chem. **111**, 3059–3065 (2007)

Gong, K., Shi, T., Ramachandran, P.A., Hutchenson, K.W., Subramaniam, B.: Adsorption/desorption studies of 224-Trimethylpentane in β-zeolite and mesoporous materials using a tapered element oscillating microbalance (TEOM). Ind. Eng. Chem. Res. **48**, 9490–9497 (2009)

Groen, J.C., Peffer, L.A.A., Moulijn, J.A., Ramirez, J.P.: Mesoporosity development in ZSM-5 zeolite upon optimized desilication conditions in alkaline medium. Colloids Surf. A, Physicochem. Eng. Asp. **241**, 53–58 (2004a)

Groen, J.C., Peffer, L.A.A., Moulijn, J.A., Ramirez, J.P.: On the introduction of intracrystalline mesoporosity in zeolites upon desilication in alkaline medium. Microporous Mesoporous Mater. **69**, 29–34 (2004b)

Groen, J.C., Zhu, W.D., Brouwer, S., Huynink, S.J., Kapteijn, F., Moulijn, J.A., Ramirez, J.P.: Direct demonstration of enhanced diffusion in mesoporous ZSM-5 zeolite obtained via controlled desilication. J. Am. Chem. Soc. **129**, 355–360 (2007)

Gunadi, A., Brandani, S.: Diffusion of linear paraffins in NaCaA studied by the ZLC method. Microporous Mesoporous Mater. **90**, 278–283 (2006)

Holmberg, B.A., Wang, H.T., Norbeck, J.M., Yan, Y.S.: Controlling size and yield of zeolite Y nanocrystals using tetramethylammonium bromide. Microporous Mesoporous Mater. **59**, 13–28 (2003)

Jacobsen, C.J.H., Madsen, C., Janssens, T.V.W., Jakobsen, H.J., Skibsted, J.: Zeolites by confined space synthesis—characterization of the acid sites in nanosized ZSM-5 by ammonia desorption and 27Al/29Si-MAS NMR spectroscopy. Microporous Mesoporous Mater. **39**, 393–401 (2000)

Jiang, M., Eić, M.: Transport properties of ethane, butanes and their binary mixtures in MFI-type zeolite and zeolite-membrane samples. Adsorption **9**, 225–234 (2003)

Jung, J.S., Park, J.W., Seo, G.: Catalytic cracking of n-octane over alkali-treated MFI zeolites. Appl. Catal. A, Gen. **288**, 149–157 (2005)

Kang, Y.F., Du, X.D., Liu, Z.J., Cui, Q., Wang, H.Y., Yao, H.Q.: Adsorption/desorption and diffusion property of n-heptane on 5A molecular sieves under high temperature. J. Chem. Eng. Chin. Univ. **25**, 172–175 (2011)

Karger, J., Ruthven, D.M.: Diffusion in Zeolites and Other Microporous Solids. Wiley, New York (1992)

Perez-Ramirez, J., Christenser, C.H., Egeblae, K., Christensen, C.H., Groen, J.C.: Hierarchical zeolites: enhanced utilisation of microporous crystals in catalysis by advances in materials design. Chem. Soc. Rev. **37**, 2530–2542 (2008)

Serrano, D.P., Aguado, J., Escola, J.M., Rodriguez, J.M., Peral, A.: Effect of the organic moiety nature on the synthesis of hierarchical ZSM-5 from silanized protozeolitic units. J. Mater. Chem. **18**, 4210–4218 (2008)

Serrano, D.P., Aguado, J., Morales, G., Rodriguez, J.M., Peral, A., Thommes, M., Epping, J.D., Chmelka, B.F.: Molecular and meso- and macroscopic properties of hierarchical nanocrystalline ZSM-5 zeolite prepared by seed silanization. Chem. Mater. **21**, 641–654 (2009)

Soler-Illia, G.J., Sanchez, C., Lebeau, B., Patarin, J.: Chemical strategies to design textured materials: from microporous and mesoporous oxides to nanonetworks and hierarchical structures. Chem. Rev. **102**, 4093–4138 (2002)

Su, L.L., Liu, L., Zhuang, J.Q., Wang, H.X., Li, Y.G., Shen, W.J., Xu, Y.D., Bao, X.H.: Creating mesopores in ZSM-5 zeolite by alkali treatment: a new way to enhance the catalytic performance of methane dehydroaromatization on MoHZSM-5 catalysts. Catal. Lett. **91**, 155–167 (2003)

Tao, Y.S., Kanoh, H., Abrams, L., Kaneko, K.: Mesopore-modified zeolites: preparation, characterization, and applications. Chem. Rev. **106**, 896–910 (2006)

van Donk, S., Janssen, A.H., Bitter, J.H., Jong, K.P.: Generation, characterization, and impact of mesopores in zeolite catalysts. Catal. Rev. **45**, 297–319 (2003)

Vinh-Thang, H., Huang, Q.L., Ungureanu, A., Eic, M., Trong-On, D., Kaliaguine, S.: Structural and diffusion characterizations of steam-stable mesostructured zeolitic ul-ZSM-5 materials. Langmuir **22**, 4777–4786 (2006)

Xiao, F.S., Wang, L.F., Yin, C.Y., Lin, K.F., Yan, D., Li, J.X., Xu, R.R., Su, D.S., Schlogl, R., Yokoi, T., Tatsumi, T.: Catalytic properties of hierarchical mesoporous zeolites templated with a mixture of small organic ammonium salts and mesoscale cationic polymers. Angew. Chem. Int. Ed. **45**, 3090–3093 (2006)

Xue, Z., Zhang, T., Ma, J., Miao, H., Fan, W., Zhang, Y., Li, R.: Accessibility and catalysis of acidic sites in hierarchical ZSM-5 prepared by silanization. Microporous Mesoporous Mater. **151**, 271–276 (2012)

Zhao, L., Shen, B.J., Gao, J.S., Xu, C.M.: Investigation on the mechanism of diffusion in mesopore structured ZSM-5 and improved heavy oil conversion. J. Catal. **258**, 228–234 (2008)